Robust immune responses after one dose of BNT162b2 mRNA vaccine dose in SARS-CoV-2 experienced individuals

Authors: Marie I. Samanovic[1†], Amber R. Cornelius[1†], Sophie L. Gray-Gaillard[1], Joseph Richard Allen[1], Trishala Karmacharya[1], Jimmy P. Wilson[1], Sara Wesley Hyman[1], Michael Tuen[1], Sergei B. Koralov[2], Mark J. Mulligan[1*], Ramin Sedaghat Herati[1*]

Affiliations:
[1]NYU Langone Vaccine Center, Department of Medicine, New York University Grossman School of Medicine; New York, NY, USA.
[2]Department of Pathology, New York University School of Medicine; New York, NY, USA.

[†]These authors contributed equally to this work.
[*]These authors contributed equally to this work.

*Corresponding authors:
Ramin Sedaghat Herati
Email: ramin.herati@nyulangone.org

Mark J. Mulligan
Email: mark.mulligan@nyulangone.org

One Sentence Summary: Prior history of COVID-19 affects adaptive immune responses to mRNA vaccination.

ABSTRACT

The use of COVID-19 vaccines will play a major role in helping to end the pandemic that has killed millions worldwide. COVID-19 vaccine candidates have resulted in robust humoral responses and protective efficacy in human trials, but efficacy trials excluded individuals with prior diagnosis of COVID-19. As a result, little is known about how immune responses induced by mRNA vaccine candidates differ in individuals who recovered from COVID-19. Here, we evaluated longitudinal immune responses to two-dose BNT162b2 mRNA vaccination in 13 adults who recovered from COVID-19, compared to 19 adults who did not have prior COVID-19 diagnosis. Consistent with prior studies of mRNA vaccines, we observed robust cytotoxic CD8 T cell responses in both cohorts. Furthermore, SARS-CoV-2-naive individuals had progressive increases in humoral and antigen-specific antibody-secreting cell (ASC) responses following each dose of vaccine, whereas SARS-CoV-2-experienced individuals demonstrated strong humoral and antigen-specific ASC responses to the first dose but muted responses to the second dose of the vaccine for the time points studied. Together, these data highlight the relevance of immunological history for understanding vaccine immune responses and may have significant implications for personalizing mRNA vaccination regimens used to prevent COVID-19.

INTRODUCTION

SARS-CoV-2 has caused hundreds of millions of infections and millions of deaths worldwide *(1)*. Although repeated infection has been described in isolated cases *(2, 3)*, resolution of SARS-CoV-2 infection was associated with reduced susceptibility to re-infection in animal models *(4)* and in humans *(5)*. However, it remains unknown how long this protection lasts. A number of promising vaccine candidates have emerged including mRNA vaccines, vector-based vaccines, and protein-adjuvant vaccines *(6)*. Maintenance of protective immune responses via vaccines will be important for preventing *de novo*, or recurrent, infection with SARS-CoV-2 virus.

Identification of protective correlates of immunity will be critical to predicting susceptibility to SARS-CoV-2 infection. Humoral responses have been identified as a correlate of immunity for a variety of pathogens *(7)*. In the setting of SARS-CoV-2 infection in non-human primates, humoral responses conferred protection, and T cell responses were partially protective in the setting of waning antibody titers *(8)*. Indeed, studies with mRNA vaccine candidates against SARS-CoV-2 have induced robust humoral responses against SARS-CoV-2 in animal models *(9–11)* and in humans *(12–17)* and were efficacious in large-scale clinical trials *(18, 19)*. In addition to humoral responses, mRNA vaccines induced type 1 responses in CD4 T cells following mRNA vaccination, as evidenced by ELISpot and intracellular cytokine staining for interferon gamma and IL-2 *(13, 14)*. However, the full spectrum of immune responses to the vaccines have not been evaluated.

Memory is the hallmark of adaptive immune responses and typically results in faster resolution of infection upon re-exposure. Moreover, mice with a particular immunological history responded differently to pathogens compared to mice who had not had prior infections *(20, 21)*. Immunological history can radically shape subsequent immune responses in other ways. For example, influenza susceptibility has been linked to strain-specific exposure from decades earlier *(22, 23)*. Moreover, non-neutralizing antibody responses to acute dengue infection are a risk factor for antibody-dependent disease enhancement for serodiscordant strains *(24, 25)*. These, and other examples from the literature *(26)*, further highlight the importance for understanding immunological history in the context of COVID-19 vaccines. Moreover, large-scale clinical trials excluded individuals with a prior diagnosis of COVID-19, thereby leaving an unexplored gap in our understanding of vaccine responses in SARS-CoV-2-experienced individuals. Indeed, given the scope of the pandemic, addressing this gap in knowledge will be relevant to hundreds of millions of recovered individuals worldwide.

Here, our goal was to evaluate the effects of prior history of COVID-19 on the immune response to mRNA vaccination. Following COVID-19, humoral and cellular immune responses persist *(27–29)*, but little is known about the effects of prior COVID-19 on subsequent exposure to SARS-CoV-2 proteins. In an observational study, we longitudinally evaluated and compared adults who were SARS-CoV-2-naive to those who were SARS-CoV-2-experienced following mRNA vaccination. Using unbiased high-dimensional flow cytometry analyses, we found robust cytotoxic CD8 T cell responses to vaccination but relatively muted CD4 responses. However, further analysis revealed subtle differences between cohorts. We found evidence for altered antigen-specific ASC induction in circulation and altered humoral responses to vaccination depending on prior history of COVID-19. Better understanding of the effects of prior COVID-19 on the

immune responses to COVID-19 vaccines will improve our ability to predict susceptibility and enable personalized vaccine strategies for maintenance of immunity.

RESULTS

Robust T cell responses to mRNA vaccination

Prior immune history can affect subsequent responses to antigen *(20)*. To test the effects of immunological history in the setting of COVID-19, we recruited 13 individuals who had laboratory-confirmed COVID-19 (hereafter labeled SARS-CoV-2-experienced) and 19 individuals who did not have documented COVID-19 (hereafter labeled SARS-CoV-2-naive). Participants' ages ranged from 24 to 65, with a median age of 39 for naive adults and 43.5 for SARS-CoV-2-experienced individuals (table S1). All SARS-CoV-2-experienced adults had mild COVID-19 or asymptomatic infection. Two individuals were infected with SARS-CoV-2 within 30 days prior to vaccination, whereas the remaining 11 were at least six months beyond diagnosis of COVID-19. For these two cohorts, all participants received two doses of the BNT162b2 mRNA vaccine in accordance with FDA's Emergency Use Authorization, and peripheral immune responses assessed before and after each dose of vaccine (**Fig. 1A**). Samples were categorized as Baseline, Post 1st dose (6–9 days after vaccination), Pre 2nd dose (immediately prior to second vaccination and ~21 days since initial vaccination), Post 2nd dose (6–9 days after second vaccination), and One month post 2nd dose (~4 weeks after second vaccination) (fig. S1A).

To determine the phenotype of circulating T cells responding to vaccination, we performed high-dimensional spectral flow cytometry longitudinally for all participants (fig. S1B, table S2). We initially reasoned that T cell responses would be evident following the second dose, thus we performed cluster analysis *(30)* and tSNE representation of all non-naive CD8 T cells (**Fig. 1B**). Of the 29 clusters identified, only Cluster 12 increased in abundance at the Post 2nd dose time point compared to Pre 2nd dose (**Fig. 1C**, and fig. S1, C and D). Cells in Cluster 12 expressed high levels of multiple proteins associated with activation, including Ki67, CD38, and ICOS (**Fig. 1D**). We next assessed these cells longitudinally using manual gating for Ki67 and CD38. Indeed, we found that vaccination was associated with robust induction of Ki67+CD38+ CD8 T cells one week after each vaccination (**Fig. 1**, **E** and **F**), which was consistent with prior reports of robust induction of cytotoxic T cells after vaccination *(31)*. Compared to baseline Ki67+CD38+ CD8 T cell frequencies, the first vaccination induced a median 1.7-fold increase for SARS-CoV-2-naive and 1.7-fold increase for SARS-CoV-2-experienced individuals. However, compared with the Pre 2nd dose time point, the second vaccination induced a 2.6-fold and 3.3-fold increase in SARS-CoV-2-naive and -experienced subjects, respectively, at one week post second dose. We also considered whether there might be differential timing of CD8 T cell responses between the two cohorts, but analysis of time as a continuous variable did not identify a consistent pattern (fig. S1, E and F). Moreover, Ki67+CD38+ CD8 T cells expressed high levels of Granzyme B, suggesting strong cytotoxic potential, and responded with memory kinetics to repeat exposure to SARS-CoV-2 antigens (fig. S1, G and H). Together, these data show that mRNA vaccination was associated with cytotoxic CD8 T cell responses in both cohorts.

We next asked if similar changes were evident in circulating CD4 T cells. Here, cluster analysis and tSNE representation of non-naive CD4 T cells identified 22 clusters, two of which increased in abundance after the second dose of vaccine (**Fig. 1G**, and fig.

S1I). Of these responding clusters, Cluster 13 was associated with high expression of Ki67, CD38, and ICOS (fig. S1, J and K). Indeed, longitudinal analysis revealed induction of Ki67+CD38+ CD4 T cells following immunization in the SARS-CoV-2-naive adults, with a 1.9-fold increase after first vaccination compared to baseline and a 1.4-fold increase at Post 2nd dose compared to Pre 2nd dose time points. In contrast, we observed muted CD4 responses in SARS-CoV-2-experienced adults (**Fig. 1**, **H** and **I**). We considered whether there might be differential timing of CD4 T cell responses between the two cohorts but again did not identify a consistent pattern (fig. S1, L and M).

We next asked if these activated CD4 and CD8 T cell responses were correlated. Indeed, we found strong positive correlation between activated CD4 and CD8 responses after the first dose of vaccine and a weak correlation after the second dose of vaccine in SARS-CoV-2-naive adults (**Fig. 1, J** and **K**). In contrast, activated CD4 and CD8 responses in SARS-CoV-2-experienced adults had a modest correlation after the first dose and no correlation after the second dose of vaccine. We also considered other demographic variables in the analysis. Aging has been associated with reduced vaccine immunogenicity and effectiveness. Indeed, COVID-19 mortality increases with age *(32)*, and it remains unclear how well COVID-19 vaccine candidates perform in older adults *(33)*. Here, we observed no correlation with age in activated CD8 T cell responses but found negative correlations in activated CD4 responses with participant age following primary and second vaccinations (**Fig. 1L**, and fig. S1N). These results indicated the potential for reduced CD4 T cell responses to vaccination with aging and underscored the need for additional studies to fully understand effects of aging on mRNA vaccine immune responses.

Differential induction of cTfh by infection history

Most vaccines are thought to confer protection via induction of a class-switched, affinity-matured antibody response *(7)*. Moreover, maturation of B cell responses within germinal centers requires help from CD4+ T follicular cells (Tfh) *(34, 35)*. However, lymphoid tissue is challenging to routinely study in humans. We and others, focused on a circulating Tfh-like subset with similar phenotypic, transcriptional, epigenetic, and functional characteristics to lymphoid Tfh *(36–40)*. Indeed, we previously found that vaccination induced antigen-specific ICOS+CD38+ circulating Tfh (cTfh) which correlated with plasmablast responses and demonstrated memory kinetics *(41)*. Furthermore, other studies identified cTfh responses in non-human primates following mRNA vaccination for influenza *(42)*. However, cTfh have not been evaluated in humans following mRNA vaccination for protection against COVID-19.

Given the subtle differences in T cell responses following mRNA vaccination between cohorts (**Fig. 1**), we next asked if cTfh responses to vaccination were similarly induced with each vaccination. Antigen-specific ICOS+CD38+ cTfh were found in circulation 1–2 weeks after yellow fever vaccination *(43)*, which was later than observed with influenza vaccine *(41)*, thus we scrutinized all time points for evidence of cTfh responses. Indeed, ICOS+CD38+ cTfh cells increased following vaccination in SARS-CoV-2-naive adults and peaked one week after the second vaccine dose (**Fig. 2, A** and **B**). In contrast, SARS-CoV-2-experienced adults did not show similar induction of cTfh cells following either dose of the vaccine. In prior studies, antigen-specific ICOS+CD38+

cTfh were shown to express CXCR3 following influenza vaccination *(39, 41)*. Here, we identified an 2.3-fold induction of CXCR3+ cells among ICOS+CD38+ cTfh cells in SARS-CoV-2-experienced adults after the first vaccine dose, in contrast to 1.7-fold increase among SARS-CoV-2-naive adults after the first dose (**Fig. 2**, **C** and **D**). There was minimal change in CXCR3 expression in ICOS+CD38+ cTfh one week after the second dose of vaccine in either cohort. Together, these data demonstrate that prior history of SARS-CoV-2 exposure affects cTfh response to mRNA vaccination.

In high-dimensional analyses of non-naive CD4 (fig. S1J), the ICOS+CD38+ cTfh cells comprised just 8% of the cluster 13 one week after each vaccination and were more commonly part of other clusters (i.e. ~44% were identified as cluster 16). Thus, we asked if the cTfh response correlated with the Ki67+CD38+ CD4 response. Indeed, ICOS+CD38+ cTfh from SARS-CoV-2-naive adults correlated positively with Ki67+CD38+ CD4 T cells for the fold-change at Post 1st dose compared to baseline (**Fig. 2E**) and at Post 2nd dose compared to Pre 2nd dose (**Fig. 2F**). In contrast, SARS-CoV-2-experienced adults had a positive correlation after the first dose and did not have a correlation after the second dose. We also found negative correlations with age that was similar between cohorts, similar to what was observed for activated CD4 responses (**Fig. 1**).

We also evaluated other well-established cellular correlates of the humoral response such as plasmablasts *(42)*, CD21lo B cells *(44)*, and CD71+ B cells *(45)* but found little or no induction of these subsets in either cohort longitudinally (fig. S2, C to I). Plasma CXCL13, which has been reported as a plasma biomarker of early germinal center activity *(46)*, also did not change following vaccination in either cohort (fig. S2J) but was elevated in an independent cohort of adults with acute COVID-19 (fig. S2K).

Altogether, we found weak induction of ICOS+CD38+ cTfh with subtle differences between cohorts. Indeed, while the ICOS+CD38+ cTfh frequency continued to increase in the SARS-CoV-2-naive adults there was no evidence of induction of cTfh in SARS-CoV-2-experienced adults over the course of the vaccination series. Given that Tfh provide help to B cells, these data provoked the question as to whether B cell responses also differed by prior history of COVID-19.

Induction of SARS-CoV-2-specific ASC in circulation after vaccination

We observed subtle differences in induction of ICOS+CD38+ cTfh following vaccination based on prior history of COVID-19 (**Fig. 2**). Thus we next asked if antigen-specific B cell responses induced by vaccination are influenced by prior exposure to the virus. To test this, we performed ELISpot analyses of antibody-secreting cells for reactivity against SARS-CoV-2 proteins one week after each vaccine dose.

Given the persistence of SARS-CoV-2-reactive B cells in individuals who recovered from COVID-19 *(28)*, we expected to find a stronger antigen-specific ASC response in SARS-CoV-2-experienced adults than SARS-CoV-2-naive adults after the first dose of vaccine. Indeed, after the first dose of vaccine, SARS-CoV-2-naive adults had few SARS-CoV-2-specific ASCs detected, whereas SARS-CoV-2-experienced adults had stronger IgG-secreting ASC responses to RBD, S1, and S2 proteins (**Fig. 3**, **A** to **C,** fig. S3, A and B). Moreover, IgA-secreting ASC were identified predominantly in SARS-CoV-2-experienced adults after the first vaccine dose, albeit at a lower frequency than IgG-secreting ASC (**Fig. 3D**). Few IgM-specific ASC were identified (fig. S3C).

Although global plasmablast frequencies did not change with vaccination (fig. S2, C to E), we did indeed find evidence of antigen-specific ASC responses following the first vaccine dose.

We next asked if the second vaccination also induced strong antigen-specific ASC responses in the two cohorts. Indeed, the second dose of vaccine robustly induced S1- and RBD-reactive ASC in SARS-CoV-2-naive adults (**Fig. 3**, **E** to **I**). In contrast, however, the second dose of vaccine induced similar, or weaker, ASC responses in SARS-COV-2-experienced adults approximately one week after vaccination for all three SARS-CoV-2 antigens tested (fig. S3D). Antigen-specific ASC induction was correlated by isotype and antigen in SARS-CoV-2-experienced adults one week after the first vaccination and SARS-CoV-2-naive one week after the second vaccination (**Fig. 3**, **J** and **K**, fig. S3, E to H). However, correlations by isotype and antigen were not observed in the SARS-CoV-2-experienced adults following the second vaccination.

Together, these data demonstrated increased induction of antigen-specific ASC responses with repeated vaccination in SARS-CoV-2-naive adults, whereas fewer antigen-specific ASC were observed in circulation with repeated vaccination in SARS-CoV-2-experienced adults.

Humoral responses differ by history of COVID-19

ASC induction differed by prior history of COVID-19 (**Fig. 3**), thus we next asked whether humoral responses were affected by prior history of COVID-19. To test this, we first assessed antibody responses to the S1 subunit of the Spike protein *(47)*. As previously demonstrated *(28)*, anti-S1 IgG antibodies were detectable in individuals who had recovered from COVID-19 and were not detectable in those who were SARS-CoV-2-naive at baseline (median titers 6232 and 25, respectively; P=7.9x10^{-6}; Wilcoxon test) (**Fig. 4A**, and fig. S4A). Following first dose immunization, SARS-CoV-2-experienced adults had a median fold-change of 54 whereas SARS-CoV-2-naive adults had a median fold-change of 3.2 (P=0.007; Wilcoxon test). However, after second dose immunization, SARS-CoV-2-experienced adults had a median fold-change of 1.4 whereas the SARS-CoV-2-naive adults had a fold-change of 10 (P=0.001; Wilcoxon test). Indeed, the two cohorts had similar anti-S1 IgG titers one week after the second vaccination (P=0.06; Wilcoxon test; fig. S4B) as well as one month after the second vaccination (P=0.19; Wilcoxon test). A similar pattern was observed for anti-S1 IgA titers (**Fig. 4B**), and, as expected, vaccination did not affect levels of anti-nucleocapsid antibodies (fig. S4C). The change in titer in SARS-CoV-2-experienced adults was inversely correlated with their titer at baseline (fig. S4D). Thus, these data demonstrate rapid and robust humoral responses after initial vaccination in both cohorts but minimal further increase in SARS-CoV-2-experienced adults after the second vaccine dose.

In a subset of participants, we asked if neutralizing antibodies were induced following immunization. We observed low titers of neutralizing antibodies at baseline in SARS-CoV-2-experienced adults, whereas sera from SARS-CoV-2-naive adults did not have detectable neutralizing antibodies (**Fig. 4, C** and **D**, and fig. S4E). Following the first immunization, SARS-CoV-2-experienced adults had a rapid increase in neutralizing antibody titers to median 6429, whereas SARS-CoV-2-naive adults achieved a titer of 10 (P=0.015; Wilcoxon test). As observed with total binding anti-S1 antibodies, subsequent neutralizing antibody titers were largely unchanged after second

vaccination, at least over the observed period, in SARS-CoV-2-experienced adults, whereas the neutralizing titers in SARS-CoV-2-naive adults continued to increase. Neutralizing titers were similar one week after the second vaccination (fig. S4F).

Antibody avidity has been used to assess affinity maturation following vaccination *(48–50)*. To assess avidity, urea wash ELISA was performed for anti-S1 IgG antibodies on serum samples longitudinally. In SARS-CoV-2-naive adults, avidity continued to increase steadily over the measured time points (**Fig. 4E**), including at one month post 2nd dose when antibody titers had plateaued. All SARS-CoV-2-experienced adults assayed had relatively high-avidity antibodies at baseline, but, in contrast to SARS-CoV-2-naive adults, avidity decreased in 4 of 5 participants over time and with second vaccination, which was may have been due to the induction of new, low avidity humoral responses that had not undergone germinal center maturation.

All together, these data demonstrated pronounced differences in humoral responses based on prior history of COVID-19.

DISCUSSION

Prior studies have demonstrated the importance of humoral and cellular responses for susceptibility to COVID-19 *(8)*. Better understanding of factors that affect immune responses will be critical to the design of next generation SARS-CoV-2 vaccines and their optimal use. Here, we observed subtle differences in cellular responses and more pronounced differences in humoral responses between individuals naive to SARS-CoV-2 and those who had recovered from SARS-CoV-2 infection. Both cohorts had similar robust CD8 T cell responses to vaccination, which was typified by co-expression of Ki67 and CD38, whereas CD4 T cell responses were generally more muted. In the immune response to mRNA vaccination, reactive T cell responses were evident following vaccination, particularly in CD8 T cells. Among CD4 responses, ICOS+CD38+ cTfh expressing CXCR3 increased following vaccination in both cohorts, but whereas vaccination induced a sharp rise in this subset in SARS-CoV-2-experienced individuals, a more gradual increase in this subset was observed in SARS-CoV-2-naive individuals. Furthermore, antigen-specific B cell responses differed by cohort as well. SARS-CoV-2-experienced adults had more antigen-specific ASC in circulation one week after the first vaccination compared to SARS-CoV-2-naive adults, but the frequency of antigen-specific ASC after second vaccination did not increase in previously infected individuals, unlike the SARS-CoV-2-naive adults. Additionally, prior history of COVID-19 was associated with 100- to 1000-fold increase in anti-Spike IgG antibody titers following the first vaccination, with limited increase upon the second vaccination, whereas antibody titers increased steadily over time in SARS-CoV-2-naive adults.

Prior studies have evaluated adaptive immune responses to mRNA vaccination *(31)*. Indeed, potent induction of cytotoxic T cell responses was observed in animal models *(31)*. Consistent with these studies, here we also observed robust induction of cytotoxic CD8 T cell responses following vaccination. Although we did not observe Ki67+CD38+ CD4 T cell responses in either cohort, other reports have identified antigen-specific CD4 T cell responses following mRNA vaccination *(14)*, thus indicating establishment of CD4 T cell responses following vaccination. Furthermore, we evaluated cTfh responses which correlated with B cell and humoral responses in prior studies *(37–39)*. We found induction of CXCR3+ ICOS+CD38+ cTfh with vaccination in both cohorts, suggesting establishment of memory Tfh populations following vaccination. Indeed, two prior studies evaluated mRNA vaccination for influenza in humans and non-human primates and found robust induction of ICOS+CXCR3+PD-1+ cTfh responses and neutralizing antibodies *(42, 51)*, which was similar to our observations in the current study. Thus, our data are overall consistent with prior studies of the establishment of robust adaptive immune responses following mRNA vaccination, particularly in SARS-CoV-2-naive adults.

However, differences in immune responses were observed when comparing adults who were naive to SARS-CoV-2 to those who had recovered from SARS-CoV-2 infection. Notably, humoral responses were robust after the first vaccination but more muted after the second vaccination in SARS-CoV-2-experienced adults, and this difference was evident in anti-Spike IgG, IgA, and neutralizing antibodies. Several possibilities may explain these differences. For example, the early plateau in humoral responses could indicate altered B cell differentiation away from antigen-specific plasma

cells, which would be consistent with the relatively poor ASC responses in SARS-CoV-2-experienced adults after the second dose. In addition, the reduction in antigen-specific ASC may have also altered trafficking of ASC following repeat vaccination, perhaps shifting the peak ASC response earlier than was assessed here. Another possibility is that the very high titers of anti-S1 IgG responses may restrict antigen availability for stimulation of non-memory B cell clones following subsequent vaccine doses. Indeed, there was a strong negative correlation between the baseline anti-S1 IgG titer and the fold-change in anti-S1 IgG titers after first vaccination. Furthermore, differences between cohorts could arise from differences in APC priming, as the duration of the dysregulation of innate immune responses in the setting of COVID-19 *(52)* remains unknown. Future studies will be needed to better understand adaptive immune responses to COVID-19 mRNA vaccination, which will have direct implications for durable, effective protection from infection.

Ideally, vaccination will result in durable protection from infection. During the study period, both SARS-CoV-2-naive and SARS-CoV-2-experienced adults achieved comparable total binding IgG and neutralizing antibody titers, which appeared to peak one week after second vaccination, consistent with published reports of humoral responses to mRNA vaccination *(12, 18)*. Moreover, humoral responses continued to qualitatively change in affinity despite the plateau. In SARS-CoV-2-naive adults, affinity increased over time, which may reflect germinal center-related affinity maturation *(11, 53)*. In contrast, SARS-CoV-2-experienced adults had reduction in affinity over time, presumably reflecting the contribution of *de novo* B cell responses that had not undergone affinity maturation, rather than loss of high-affinity antibodies. Longer follow-up will be needed to determine whether humoral responses continue to quantitatively or qualitatively differ between these two cohorts.

Together, these results highlight the importance of understanding prior immunological experience on the subsequent immune response to COVID-19 mRNA vaccines. Future studies will be needed to determine whether such personalized vaccination regimens will deliver durable, protective immunity to infection by the SARS-CoV-2 virus.

MATERIALS AND METHODS

Study Design

Thirty-two adults (19 SARS-CoV-2-naïve and 13 SARS-CoV-2-experienced) provided written consent for enrollment with approval from the NYU Institutional Review Board (protocols 18-02035 and 18-02037).

Blood samples processing and storage

Venous blood was collected by standard phlebotomy. Blood collection occurred at baseline, approximately one week after first vaccination ("Post 1st dose"), prior to the second vaccination ("Pre 2nd dose"), one week after the second vaccination ("Post 2nd dose"), and one month after the second vaccination ("One month post 2nd dose"), as depicted in fig. S1A. Peripheral blood mononuclear cells (PBMC) were isolated from heparin vacutainers (BD Biosciences) that were stored overnight at room temperature (RT), followed by processing using Sepmates (Stem Cell, Inc) in accordance with the manufacturer's recommendations. Serum was collected in SST tubes (BD Biosciences) and frozen immediately at -80^{o}C.

ELISA

Direct ELISA was used to quantify antibody titers in participant serum. Ninety-six well plates were coated with 1 µg/ml S1 protein (100 µl/well) or 0.1 µg/ml N protein diluted in PBS and were then incubated overnight at 4°C (Sino Biological Inc., 40591-V08H and 40588-V08B). Plates were washed four times with 250 µl of PBS containing 0.05% Tween 20 (PBS-T) and blocked with 200 µl PBS-T containing 4% non-fat milk and 5% whey, as blocking buffer at RT for 1 hour. Sera were heated at 56°C for 1 hour prior to use. Samples were diluted to a starting concentration of 1:50 (S1), or 1:100 (N) were first added to the plates and then serially diluted 1:3 in blocking solution. The final volume in all wells after dilution was 100 µl. After a 2-hour incubation period at RT, plates were washed four times with PBS-T. Horseradish-peroxidase conjugated goat-anti human IgG, IgM, and IgA (Southern BioTech, 2040-05, 2020-05, 2050-05) were diluted in blocking buffer (1:2000, 1:1000, 1:1000, respectively) and 100 µl was added to each well. Plates were incubated for 1 hour at RT and washed four times with PBS-T. After developing for 5 min with TMB Peroxidase Substrate 3,3′,5,5′-Tetramethylbenzidine (Thermo Scientific), the reaction was stopped with 1M sulfuric acid or 1N hydrochloric acid. The optical density was determined by measuring the absorbance at 450 nm on a Synergy 4 (BioTek) plate reader.

In order to summarize data collected on individuals, the area under the response curve was calculated for each sample and end point titers were normalized using replicates of pooled positive control sera on each plate to reduce variability between plates.

Avidity assay

Ninety-six well plates were coated with 0.1 µg/ml S1 protein (100 µl/well) diluted in PBS overnight at 4°C (Sino Biological). Plates were washed four times with 250 µl of PBS

containing 0.05% Tween 20 (PBS-T) and blocked with 200 µl PBS-T containing 4% non-fat milk and 5% whey, as blocking buffer at RT for 1 hour. Sera were heated at 56°C for 1 hour prior to use. Samples were diluted to a starting concentration of 1:50 and added to the plates in quadruplicate and then serially diluted 1:3 in blocking solution. The final volume in all wells after dilution was 100 µl. After a 2-hour incubation period at RT, plates were washed four times with PBS-T. PBS was then added to two dilution replicate sets and 6 M Urea to the other two dilution replicate sets. Plates were incubated for 10 min at RT before washing four times with PBST. Antibodies were detected and plates were developed and read as described in above ELISA assays.

Avidity was calculated by dividing the dilutions that gave an Optical Density value of 0.5 (Urea treatment/no Urea). Scores with theoretical values between 0 and 100% were generated.

Antibody-secreting cell ELISpot Assays

A direct enzyme-linked immunospot (ELISpot) assay was used to determine the number of SARS-CoV-2 spike protein subunit S1-, S2-, and receptor-binding domains (RBD)-specific IgG, IgA, and IgM ASCs in fresh PBMCs. Ninety-six well ELISpot filter plates (Millipore, MSHAN4B50) were coated overnight with 2 µg/mL recombinant S1, S2, or RBD (Sino Biological Inc., 40591-V08H, 40590-V08B, and 40592-V08H), or 10 µg/mL of goat anti-human IgG/A/M capture antibody (Jackson ImmunoResearch Laboratory Inc., 109-005-064). Plates were washed 4 times with 200 µl PBS-T and blocked for 2 hours at 37°C with 200 µl RPMI 1640 containing 10% fetal calf serum (FCS), 100 units/ml of penicillin G, and 100 µg/ml of streptomycin (Gibco), referred to as complete medium. Fifty µl of cells in complete medium at $10x10^6$ cells/ml were added to the top row of wells containing 150 µl complete medium and 3-fold serial diluted 3 times. Plates were incubated overnight at 37°C with 5% CO_2. Plates were washed 1 time with 200 µl PBS followed by 4 times with 200 µl PBS-T. Biotinylated anti-human IgG, IgM, or IgA antibody (Jackson ImmunoResearch Laboratory Inc., 709-065-098, 109-065-129, 109-065-011) were diluted 1:1000 in PBS-T with 2% FCS (Ab diluent) and 100 µl was added to wells for 2 hours at RT or overnight at 4^oC. Plates were washed 4 times with 200 µl PBS-T and incubated with 100 µl of Avidin-D-HRP conjugate (Vector Laboratories, A-2004) diluted 1:1000 in Ab diluent for 1 hour at RT. Plates were washed 4 times with 200 µl PBS-T and 100ml of AEC substrate (3 amino-9 ethyl-carbazole; Sigma Aldrich, A-5754) was added. Plates were incubated at RT for 5 minutes and rinsed with water to stop the reaction. Developed plates were scanned and analyzed using an ImmunoSpot automated ELISpot counter (Cellular Technology Limited).

SARS-CoV-2 microneutralization assay

Viral neutralization activity of serum was measured in an immunofluorescence-based microneutralization assay by detecting the neutralization of infectious virus in cultured Vero E6 cells (African Green Monkey Kidney; ATCC #CRL-1586). These cells are known to be highly susceptible to infection by SARS-CoV-2. Cells were maintained according to standard ATCC protocols. Briefly, Vero E6 cells were grown in Minimal

Essential Medium (MEM) supplemented with 10% heat-inactivated fetal bovine serum (FBS), 2mM L-glutamine, and 1% of MEM Nonessential Amino Acid (NEAA) Solution (Fisher #MT25025CI). Cell cultures were grown in 75 or 150 cm^2 flasks at 37°C with 5% CO_2 and passaged 2-3 times per week using trypsin-EDTA. Cell cultures used for virus testing were prepared as subconfluent monolayers. All incubations containing cells were performed at 37°C with 5% CO_2. All SARS-CoV-2 infection assays were performed in the CDC/USDA-approved BSL-3 facility in compliance with NYU Grossman School of Medicine guidelines for biosafety level 3. SARS-CoV-2 isolate USA-WA1/2020, deposited by the Centers for Disease Control and Prevention, was obtained through BEI Resources, NIAID, NIH (NR-52281, GenBank accession no. MT233526). Serial dilutions of heat-inactivated serum (56°C for 1 hour) were incubated with USA-WA1/2020 stock (at fixed $1x10^6$ PFU/ml) for 1 hour 37°C. One hundred microliters of the serum-virus mix was then added to the cells and incubated at 37°C with 5% CO_2. Twenty-four hours post-infection, cells were fixed with 10% formalin solution (4% active formaldehyde) for 1 hour, stained with an α-SARS-CoV-2 nucleocapsid antibody (ProSci #10-605), and a goat α-mouse IgG AF647 secondary antibody along with DAPI and visualized by microscopy with the CellInsight CX7 High-Content Screening (HCS) Platform (ThermoFisher) and high-content software (HCS) *(54)*.

CXCL13 detection

CXCL13 was detected using the Ella instrument (ProteinSimple) and a CXCL13 Simple Plex Cartridge (ProteinSimple, SPCKB-PS-000375) on serum diluted 1:1 in buffer according to the manufacturer's instruction.

Cellular phenotyping

Peripheral blood was collected in sodium heparin collection tubes and maintained at room temperature overnight. PBMC were isolated using the Sepmate system (STEMCELL Technologies) in accordance with manufacturer's instructions. Then, 2 to 5 million freshly isolated PBMC were resuspended in HBSS supplemented with 1% fetal calf serum (Fisher) and 0.02% sodium azide (Sigma). Cells underwent Fc-blockade with Human TruStain FcX (Biolegend) and NovaBlock (Phitonex) for 10 minutes at room temperature, followed by surface staining antibody cocktail at room temperature for 20 minutes in the dark. Cells were permeabilized with the eBioscience Intracellular Fixation and Permeabilization kit (Fisher) for 20 minutes at room temperature in the dark, followed by intracellular staining with an antibody cocktail for 1 hour at room temperature in the dark. All samples were then resuspended in 1% paraformaldehyde and acquired within three days of staining on a 5-laser Aurora cytometer (Cytek Biosciences). Antibodies, clones, and catalog numbers are available in **Table S2**. Initial data quality control was performed using FlowJo. Non-naive CD8 and CD4 T cells were analyzed in the OMIQ.ai platform (www.omiq.ai) using Phenograph clustering *(30)* with k=20 and a Euclidean distance metric, followed by tSNE projection. Heatmaps and differential cluster abundance were assessed by edgeR *(55)* via OMIQ.ai.

Bioinformatics and statistical analyses

Primary data analysis and statistical analysis were performed using the R environment (version 4.0.2) and all bioinformatics scripts are available at https://github.com/teamTfh/COVIDvaccines. Statistical tests were performed using the "rstatix" library (version 0.6.0). Use of parametric or nonparametric tests was guided by Shapiro-Wilk normality testing. A log(x+1) transformation was performed prior to significance testing for 2-sample t-tests where sample variances were unequal as identified by Levene's test. Correlation analyses were performed as nonparametric tests using Kendall's tau statistic. All tests were two-tailed tests with α=0.05. Study schematic was made with BioRender.

Supplementary Materials

Fig. S1. CD4 and CD8 T cell responses and gating strategy.

Fig. S2. Plasmablasts and CXCL13 responses to vaccinations.

Fig. S3. Poor IgG and IgA ASC responses to second dose in SARS-CoV-2 experienced participants.

Fig. S4. SARS-CoV-2-experienced individuals' robust anti-S1 binding and neutralizing antibodies responses after the first dose.

Table S1. Participant demographics.

Table S2. Antibodies used in flow cytometry experiments.

REFERENCES

1. E. Dong, H. Du, L. Gardner, An interactive web-based dashboard to track COVID-19 in real time, *Lancet Infect. Dis.* **20**, 533–534 (2020).

2. K. K.-W. To, I. F.-N. Hung, J. D. Ip, A. W.-H. Chu, W.-M. Chan, A. R. Tam, C. H.-Y. Fong, S. Yuan, H.-W. Tsoi, A. C.-K. Ng, L. L.-Y. Lee, P. Wan, E. Tso, W.-K. To, D. Tsang, K.-H. Chan, J.-D. Huang, K.-H. Kok, V. C.-C. Cheng, K.-Y. Yuen, COVID-19 re-infection by a phylogenetically distinct SARS-coronavirus-2 strain confirmed by whole genome sequencing, *Clin. Infect. Dis.* (2020), doi:10.1093/cid/ciaa1275.

3. R. Tillett, J. Sevinsky, P. Hartley, H. Kerwin, N. Crawford, A. Gorzalski, C. Laverdure, S. Verma, C. Rossetto, D. Jackson, M. Farrell, S. Van Hooser, M. Pandori, Genomic Evidence for a Case of Reinfection with SARS-CoV-2 (2020), doi:10.2139/ssrn.3680955.

4. A. Chandrashekar, J. Liu, A. J. Martinot, K. McMahan, N. B. Mercado, L. Peter, L. H. Tostanoski, J. Yu, Z. Maliga, M. Nekorchuk, K. Busman-Sahay, M. Terry, L. M. Wrijil, S. Ducat, D. R. Martinez, C. Atyeo, S. Fischinger, J. S. Burke, M. D. Slein, L. Pessaint, A. Van Ry, J. Greenhouse, T. Taylor, K. Blade, A. Cook, B. Finneyfrock, R. Brown, E.

Teow, J. Velasco, R. Zahn, F. Wegmann, P. Abbink, E. A. Bondzie, G. Dagotto, M. S. Gebre, X. He, C. Jacob-Dolan, N. Kordana, Z. Li, M. A. Lifton, S. H. Mahrokhian, L. F. Maxfield, R. Nityanandam, J. P. Nkolola, A. G. Schmidt, A. D. Miller, R. S. Baric, G. Alter, P. K. Sorger, J. D. Estes, H. Andersen, M. G. Lewis, D. H. Barouch, SARS-CoV-2 infection protects against rechallenge in rhesus macaques, *Science* **369**, 812–817 (2020).

5. V. Hall, S. Foulkes, A. Charlett, A. Atti, E. J. M. Monk, R. Simmons, E. Wellington, M. J. Cole, A. Saei, B. Oguti, K. Munro, S. Wallace, P. D. Kirwan, M. Shrotri, A. Vusirikala, S. Rokadiya, M. Kall, M. Zambon, M. Ramsay, T. Brooks, C. S. Brown, M. A. Chand, S. Hopkins, SIREN Study Group, Do antibody positive healthcare workers have lower SARS-CoV-2 infection rates than antibody negative healthcare workers? Large multi-centre prospective cohort study (the SIREN study), England: June to November 2020*bioRxiv* (2021), doi:10.1101/2021.01.13.21249642.

6. G. Forni, A. Mantovani, COVID-19 Commission of Accademia Nazionale dei Lincei, Rome, COVID-19 vaccines: where we stand and challenges ahead, *Cell Death Differ.* **28**, 626–639 (2021).

7. S. A. Plotkin, Correlates of protection induced by vaccination, *Clin. Vaccine Immunol.* **17**, 1055–1065 (2010).

8. K. McMahan, J. Yu, N. B. Mercado, C. Loos, L. H. Tostanoski, A. Chandrashekar, J. Liu, L. Peter, C. Atyeo, A. Zhu, E. A. Bondzie, G. Dagotto, M. S. Gebre, C. Jacob-Dolan, Z. Li, F. Nampanya, S. Patel, L. Pessaint, A. Van Ry, K. Blade, J. Yalley-Ogunro, M. Cabus, R. Brown, A. Cook, E. Teow, H. Andersen, M. G. Lewis, D. A. Lauffenburger, G. Alter, D. H. Barouch, Correlates of protection against SARS-CoV-2 in rhesus macaques, *Nature* **590**, 630–634 (2021).

9. K. S. Corbett, B. Flynn, K. E. Foulds, J. R. Francica, S. Boyoglu-Barnum, A. P. Werner, B. Flach, S. O'Connell, K. W. Bock, M. Minai, B. M. Nagata, H. Andersen, D. R. Martinez, A. T. Noe, N. Douek, M. M. Donaldson, N. N. Nji, G. S. Alvarado, D. K. Edwards, D. R. Flebbe, E. Lamb, N. A. Doria-Rose, B. C. Lin, M. K. Louder, S. O'Dell, S. D. Schmidt, E. Phung, L. A. Chang, C. Yap, J. M. Todd, L. Pessaint, A. Van Ry, S. Browne, J. Greenhouse, T. Putman-Taylor, A. Strasbaugh, T. A. Campbell, A. Cook, A. Dodson, K. Steingrebe, W. Shi, Y. Zhang, O. M. Abiona, L. Wang, A. Pegu, E. S. Yang, K. Leung, T. Zhou, I. T. Teng, A. Widge, I. Gordon, L. Novik, R. A. Gillespie, R. J. Loomis, J. I. Moliva, G. Stewart-Jones, S. Himansu, W. P. Kong, M. C. Nason, K. M. Morabito, T. J. Ruckwardt, J. E. Ledgerwood, M. R. Gaudinski, P. D. Kwong, J. R. Mascola, A. Carfi, M. G. Lewis, R. S. Baric, A. McDermott, I. N. Moore, N. J. Sullivan, M. Roederer, R. A. Seder, B. S. Graham, Evaluation of the mRNA-1273 Vaccine against SARS-CoV-2 in Nonhuman Primates, *N. Engl. J. Med.* (2020), doi:10.1056/NEJMoa2024671.

10. P. J. Klasse, D. F. Nixon, J. P. Moore, Immunogenicity of clinically relevant SARS-CoV-2 vaccines in nonhuman primates and humans, *Sci Adv* **7** (2021), doi:10.1126/sciadv.abe8065.

11. D. Laczkó, M. J. Hogan, S. A. Toulmin, P. Hicks, K. Lederer, B. T. Gaudette, D. Castaño, F. Amanat, H. Muramatsu, T. H. Oguin 3rd, A. Ojha, L. Zhang, Z. Mu, R. Parks, T. B. Manzoni, B. Roper, S. Strohmeier, I. Tombácz, L. Arwood, R. Nachbagauer, K. Karikó, J. Greenhouse, L. Pessaint, M. Porto, T. Putman-Taylor, A. Strasbaugh, T.-A. Campbell, P. J. C. Lin, Y. K. Tam, G. D. Sempowski, M. Farzan, H. Choe, K. O. Saunders, B. F. Haynes, H. Andersen, L. C. Eisenlohr, D. Weissman, F. Krammer, P. Bates, D. Allman, M. Locci, N. Pardi, A Single Immunization with Nucleoside-Modified mRNA Vaccines Elicits Strong Cellular and Humoral Immune Responses against SARS-CoV-2 in Mice, *Immunity* **53**, 724–732.e7 (2020).

12. M. J. Mulligan, K. E. Lyke, N. Kitchin, J. Absalon, A. Gurtman, S. Lockhart, K. Neuzil, V. Raabe, R. Bailey, K. A. Swanson, P. Li, K. Koury, W. Kalina, D. Cooper, C. Fontes-Garfias, P.-Y. Shi, Ö. Türeci, K. R. Tompkins, E. E. Walsh, R. Frenck, A. R. Falsey, P. R. Dormitzer, W. C. Gruber, U. Şahin, K. U. Jansen, Phase I/II study of COVID-19 RNA vaccine BNT162b1 in adults, *Nature* **586**, 589–593 (2020).

13. A. B. Vogel, I. Kanevsky, Y. Che, K. A. Swanson, A. Muik, M. Vormehr, L. M. Kranz, K. C. Walzer, S. Hein, A. Güler, J. Loschko, M. S. Maddur, A. Ota-Setlik, K. Tompkins, J. Cole, B. G. Lui, T. Ziegenhals, A. Plaschke, D. Eisel, S. C. Dany, S. Fesser, S. Erbar, F. Bates, D. Schneider, B. Jesionek, B. Sänger, A.-K. Wallisch, Y. Feuchter, H. Junginger, S. A. Krumm, A. P. Heinen, P. Adams-Quack, J. Schlereth, S. Schille, C. Kröner, R. de la Caridad Güimil Garcia, T. Hiller, L. Fischer, R. S. Sellers, S. Choudhary, O. Gonzalez, F. Vascotto, M. R. Gutman, J. A. Fontenot, S. Hall-Ursone, K. Brasky, M. C. Griffor, S. Han, A. A. H. Su, J. A. Lees, N. L. Nedoma, E. H. Mashalidis, P. V. Sahasrabudhe, C. Y. Tan, D. Pavliakova, G. Singh, C. Fontes-Garfias, M. Pride, I. L. Scully, T. Ciolino, J. Obregon, M. Gazi, R. Carrion, K. J. Alfson, W. V. Kalina, D. Kaushal, P.-Y. Shi, T. Klamp, C. Rosenbaum, A. N. Kuhn, Ö. Türeci, P. R. Dormitzer, K. U. Jansen, U. Sahin, BNT162b vaccines are immunogenic and protect non-human primates against SARS-CoV-2*Cold Spring Harbor Laboratory* , 2020.12.11.421008 (2020).

14. U. Sahin, A. Muik, E. Derhovanessian, I. Vogler, L. M. Kranz, M. Vormehr, A. Baum, K. Pascal, J. Quandt, D. Maurus, S. Brachtendorf, V. Lörks, J. Sikorski, R. Hilker, D. Becker, A.-K. Eller, J. Grützner, C. Boesler, C. Rosenbaum, M.-C. Kühnle, U. Luxemburger, A. Kemmer-Brück, D. Langer, M. Bexon, S. Bolte, K. Karikó, T. Palanche, B. Fischer, A. Schultz, P.-Y. Shi, C. Fontes-Garfias, J. L. Perez, K. A. Swanson, J. Loschko, I. L. Scully, M. Cutler, W. Kalina, C. A. Kyratsous, D. Cooper, P. R. Dormitzer, K. U. Jansen, Ö. Türeci, COVID-19 vaccine BNT162b1 elicits human antibody and TH1 T cell responses, *Nature* **586**, 594–599 (2020).

15. E. E. Walsh, R. W. Frenck Jr, A. R. Falsey, N. Kitchin, J. Absalon, A. Gurtman, S. Lockhart, K. Neuzil, M. J. Mulligan, R. Bailey, K. A. Swanson, P. Li, K. Koury, W. Kalina, D. Cooper, C. Fontes-Garfias, P.-Y. Shi, Ö. Türeci, K. R. Tompkins, K. E. Lyke, V. Raabe, P. R. Dormitzer, K. U. Jansen, U. Şahin, W. C. Gruber, Safety and Immunogenicity of Two RNA-Based Covid-19 Vaccine Candidates, *N. Engl. J. Med.* **383**, 2439–2450 (2020).

16. L. A. Jackson, E. J. Anderson, N. G. Rouphael, P. C. Roberts, M. Makhene, R. N. Coler, M. P. McCullough, J. D. Chappell, M. R. Denison, L. J. Stevens, A. J. Pruijssers, A. McDermott, B. Flach, N. A. Doria-Rose, K. S. Corbett, K. M. Morabito, S. O'Dell, S. D. Schmidt, P. A. Swanson 2nd, M. Padilla, J. R. Mascola, K. M. Neuzil, H. Bennett, W. Sun, E. Peters, M. Makowski, J. Albert, K. Cross, W. Buchanan, R. Pikaart-Tautges, J. E. Ledgerwood, B. S. Graham, J. H. Beigel, An mRNA Vaccine against SARS-CoV-2 - Preliminary Report, *N. Engl. J. Med.* (2020), doi:10.1056/NEJMoa2022483.

17. E. J. Anderson, N. G. Rouphael, A. T. Widge, L. A. Jackson, P. C. Roberts, M. Makhene, J. D. Chappell, M. R. Denison, L. J. Stevens, A. J. Pruijssers, A. B. McDermott, B. Flach, B. C. Lin, N. A. Doria-Rose, S. O'Dell, S. D. Schmidt, K. S. Corbett, P. A. Swanson 2nd, M. Padilla, K. M. Neuzil, H. Bennett, B. Leav, M. Makowski, J. Albert, K. Cross, V. V. Edara, K. Floyd, M. S. Suthar, D. R. Martinez, R. Baric, W. Buchanan, C. J. Luke, V. K. Phadke, C. A. Rostad, J. E. Ledgerwood, B. S. Graham, J. H. Beigel, mRNA-1273 Study Group, Safety and Immunogenicity of SARS-CoV-2 mRNA-1273 Vaccine in Older Adults, *N. Engl. J. Med.* **383**, 2427–2438 (2020).

18. L. R. Baden, H. M. El Sahly, B. Essink, K. Kotloff, S. Frey, R. Novak, D. Diemert, S. A. Spector, N. Rouphael, C. B. Creech, J. McGettigan, S. Khetan, N. Segall, J. Solis, A. Brosz, C. Fierro, H. Schwartz, K. Neuzil, L. Corey, P. Gilbert, H. Janes, D. Follmann, M. Marovich, J. Mascola, L. Polakowski, J. Ledgerwood, B. S. Graham, H. Bennett, R. Pajon, C. Knightly, B. Leav, W. Deng, H. Zhou, S. Han, M. Ivarsson, J. Miller, T. Zaks, COVE Study Group, Efficacy and Safety of the mRNA-1273 SARS-CoV-2 Vaccine, *N. Engl. J. Med.* **384**, 403–416 (2021).

19. F. P. Polack, S. J. Thomas, N. Kitchin, J. Absalon, A. Gurtman, S. Lockhart, J. L. Perez, G. Pérez Marc, E. D. Moreira, C. Zerbini, R. Bailey, K. A. Swanson, S. Roychoudhury, K. Koury, P. Li, W. V. Kalina, D. Cooper, R. W. Frenck Jr, L. L. Hammitt, Ö. Türeci, H. Nell, A. Schaefer, S. Ünal, D. B. Tresnan, S. Mather, P. R. Dormitzer, U. Şahin, K. U. Jansen, W. C. Gruber, C4591001 Clinical Trial Group, Safety and Efficacy of the BNT162b2 mRNA Covid-19 Vaccine, *N. Engl. J. Med.* **383**, 2603–2615 (2020).

20. T. A. Reese, K. Bi, A. Kambal, A. Filali-Mouhim, L. K. Beura, M. C. B??rger, B. Pulendran, R. P. Sekaly, S. C. Jameson, D. Masopust, W. N. Haining, H. W. Virgin, Sequential Infection with Common Pathogens Promotes Human-like Immune Gene Expression and Altered Vaccine Response, *Cell Host Microbe* , 713–719 (2016).

21. L. K. Beura, S. E. Hamilton, K. Bi, J. M. Schenkel, O. A. Odumade, K. A. Casey, E. A. Thompson, K. A. Fraser, P. C. Rosato, A. Filali-Mouhim, R. P. Sekaly, M. K. Jenkins, V. Vezys, W. N. Haining, S. C. Jameson, D. Masopust, Normalizing the environment recapitulates adult human immune traits in laboratory mice, *Nature* **532**, 512–516 (2016).

22. S. L. Linderman, B. S. Chambers, S. J. Zost, K. Parkhouse, Y. Li, C. Herrmann, A. H. Ellebedy, D. M. Carter, S. F. Andrews, N.-Y. Zheng, M. Huang, Y. Huang, D. Strauss, B. H. Shaz, R. L. Hodinka, G. Reyes-Terán, T. M. Ross, P. C. Wilson, R. Ahmed, J. D. Bloom, S. E. Hensley, Potential antigenic explanation for atypical H1N1

infections among middle-aged adults during the 2013-2014 influenza season, *Proc. Natl. Acad. Sci. U. S. A.* **111**, 15798–15803 (2014).

23. S. Gouma, K. Kim, M. E. Weirick, M. E. Gumina, A. Branche, D. J. Topham, E. T. Martin, A. S. Monto, S. Cobey, S. E. Hensley, Middle-aged individuals may be in a perpetual state of H3N2 influenza virus susceptibility, *Nat. Commun.* **11**, 4566 (2020).

24. T. T. Wang, J. Sewatanon, M. J. Memoli, J. Wrammert, S. Bournazos, S. K. Bhaumik, B. A. Pinsky, K. Chokephaibulkit, N. Onlamoon, K. Pattanapanyasat, J. K. Taubenberger, R. Ahmed, J. V. Ravetch, IgG antibodies to dengue enhanced for FcγRIIIA binding determine disease severity, *Science* **355**, 395–398 (2017).

25. A. E. Ngono, S. Shresta, Immune Response to Dengue and Zika, *Annu. Rev. Immunol.* **36**, 279–308 (2018).

26. W. Huisman, B. E. E. Martina, G. F. Rimmelzwaan, R. A. Gruters, A. D. M. E. Osterhaus, Vaccine-induced enhancement of viral infections, *Vaccine* **27**, 505–512 (2009).

27. A. Sette, S. Crotty, Adaptive immunity to SARS-CoV-2 and COVID-19, *Cell* **184**, 861–880 (2021).

28. J. M. Dan, J. Mateus, Y. Kato, K. M. Hastie, E. D. Yu, C. E. Faliti, A. Grifoni, S. I. Ramirez, S. Haupt, A. Frazier, C. Nakao, V. Rayaprolu, S. A. Rawlings, B. Peters, F. Krammer, V. Simon, E. O. Saphire, D. M. Smith, D. Weiskopf, A. Sette, S. Crotty, Immunological memory to SARS-CoV-2 assessed for up to 8 months after infection, *Science* **371** (2021), doi:10.1126/science.abf4063.

29. C. Rydyznski Moderbacher, S. I. Ramirez, J. M. Dan, A. Grifoni, K. M. Hastie, D. Weiskopf, S. Belanger, R. K. Abbott, C. Kim, J. Choi, Y. Kato, E. G. Crotty, C. Kim, S. A. Rawlings, J. Mateus, L. P. V. Tse, A. Frazier, R. Baric, B. Peters, J. Greenbaum, E. Ollmann Saphire, D. M. Smith, A. Sette, S. Crotty, Antigen-Specific Adaptive Immunity to SARS-CoV-2 in Acute COVID-19 and Associations with Age and Disease Severity, *Cell* **183**, 996–1012.e19 (2020).

30. J. H. Levine, E. F. Simonds, S. C. Bendall, K. L. Davis, E. A. D. Amir, M. D. Tadmor, O. Litvin, H. G. Fienberg, A. Jager, E. R. Zunder, R. Finck, A. L. Gedman, I. Radtke, J. R. Downing, D. Pe'er, G. P. Nolan, Data-Driven Phenotypic Dissection of AML Reveals Progenitor-like Cells that Correlate with Prognosis, *Cell* **162**, 184–197 (2015).

31. N. Pardi, M. J. Hogan, F. W. Porter, D. Weissman, mRNA vaccines - a new era in vaccinology, *Nat. Rev. Drug Discov.* **17**, 261–279 (2018).

32. V. Bajaj, N. Gadi, A. P. Spihlman, S. C. Wu, C. H. Choi, V. R. Moulton, Aging, Immunity, and COVID-19: How Age Influences the Host Immune Response to Coronavirus Infections?, *Front. Physiol.* **11**, 571416 (2020).

33. B. K. I. Helfand, M. Webb, S. L. Gartaganis, L. Fuller, C.-S. Kwon, S. K. Inouye, The

Exclusion of Older Persons From Vaccine and Treatment Trials for Coronavirus Disease 2019-Missing the Target, *JAMA Intern. Med.* (2020), doi:10.1001/jamainternmed.2020.5084.

34. S. Crotty, T follicular helper cell differentiation, function, and roles in disease, *Immunity* **41**, 529–542 (2014).

35. S. Crotty, T Follicular Helper Cell Biology: A Decade of Discovery and Diseases, *Immunity* **50**, 1132–1148 (2019).

36. L. A. Vella, M. Buggert, S. Manne, R. S. Herati, I. Sayin, L. Kuri-Cervantes, I. Bukh Brody, K. C. O'Boyle, H. Kaprielian, J. R. Giles, S. Nguyen, A. Muselman, J. P. Antel, A. Bar-Or, M. E. Johnson, D. H. Canaday, A. Naji, V. V. Ganusov, T. M. Laufer, A. D. Wells, Y. Dori, M. G. Itkin, M. R. Betts, E. J. Wherry, T follicular helper cells in human efferent lymph retain lymphoid characteristics, *J. Clin. Invest.* **129**, 3185–3200 (2019).

37. M. Locci, C. Havenar-Daughton, E. Landais, J. Wu, M. A. Kroenke, C. L. Arlehamn, L. F. Su, R. Cubas, M. M. Davis, A. Sette, K. Elias, I. Protocol, Investigators, C. Principal, P. Poignard, S. Crotty, E. K. Haddad, Tfh cells are highly functional and correlate with broadly neutralizing HIV antibody responses, *Immunity* **39**, 1–12 (2013).

38. R. S. Herati, M. A. Reuter, D. V. Dolfi, K. D. Mansfield, H. Aung, O. Z. Badwan, R. K. Kurupati, S. Kannan, H. Ertl, K. E. Schmader, M. R. Betts, D. H. Canaday, E. J. Wherry, Circulating CXCR5+PD-1+ response predicts influenza vaccine antibody responses in young adults but not elderly adults, *J. Immunol.* **193**, 3528–3537 (2014).

39. S.-E. Bentebibel, S. Lopez, G. Obermoser, N. Schmitt, C. Mueller, C. Harrod, E. Flano, A. Mejias, R. A. Albrecht, D. Blankenship, H. Xu, V. Pascual, J. Banchereau, A. Garcia-Sastre, A. K. Palucka, O. Ramilo, H. Ueno, Induction of ICOS+CXCR3+CXCR5+ TH cells correlates with antibody responses to influenza vaccination, *Sci. Transl. Med.* **5**, 176ra32–176ra32 (2013).

40. S.-E. Bentebibel, S. Khurana, N. Schmitt, P. Kurup, C. Mueller, G. Obermoser, A. K. Palucka, R. A. Albrecht, A. Garcia-Sastre, H. Golding, H. Ueno, ICOS(+)PD-1(+)CXCR3(+) T follicular helper cells contribute to the generation of high-avidity antibodies following influenza vaccination, *Sci. Rep.* **6**, 26494–26494 (2016).

41. R. S. Herati, A. Muselman, L. Vella, B. Bengsch, K. Parkhouse, D. Del Alcazar, J. Kotzin, S. A. Doyle, P. Tebas, S. E. Hensley, L. F. Su, K. E. Schmader, E. J. Wherry, Successive annual influenza vaccination induces a recurrent oligoclonotypic memory response in circulating T follicular helper cells, *Sci Immunol* **2** (2017), doi:10.1126/sciimmunol.aag2152.

42. G. Lindgren, S. Ols, F. Liang, E. A. Thompson, A. Lin, F. Hellgren, K. Bahl, S. John, O. Yuzhakov, K. J. Hassett, L. A. Brito, H. Salter, G. Ciaramella, K. Loré, Induction of Robust B cell responses after influenza mRNA vaccination is accompanied by circulating hemagglutinin-specific ICOS+ PD-1+ CXCR3+ T follicular helper cells, *Front. Immunol.* **8**, 1539–1539 (2017).

43. Q. DeGottardi, T. J. Gates, J. Yang, E. A. James, U. Malhotra, I.-T. Chow, Y. Simoni, M. Fehlings, E. W. Newell, H. A. DeBerg, W. W. Kwok, Ontogeny of different subsets of yellow fever virus-specific circulatory CXCR5+ CD4+ T cells after yellow fever vaccination, *Sci. Rep.* **10**, 15686 (2020).

44. D. Lau, L. Y. L. Lan, S. F. Andrews, C. Henry, K. T. Rojas, K. E. Neu, M. Huang, Y. Huang, B. DeKosky, A. K. E. Palm, G. C. Ippolito, G. Georgiou, P. C. Wilson, Low CD21 expression defines a population of recent germinal center graduates primed for plasma cell differentiation, *Science Immunology* **2**, 1–14 (2017).

45. A. H. Ellebedy, K. J. L. Jackson, H. T. Kissick, H. I. Nakaya, C. W. Davis, K. M. Roskin, A. K. McElroy, C. M. Oshansky, R. Elbein, S. Thomas, G. M. Lyon, C. F. Spiropoulou, A. K. Mehta, P. G. Thomas, S. D. Boyd, R. Ahmed, Defining antigen-specific plasmablast and memory B cell subsets in human blood after viral infection or vaccination, *Nat. Immunol.* **17**, 1226–1234 (2016).

46. C. Havenar-Daughton, M. Lindqvist, A. Heit, J. E. Wu, S. M. Reiss, K. Kendric, S. Bélanger, S. P. Kasturi, E. Landais, R. S. Akondy, H. M. McGuire, M. Bothwell, P. A. Vagefi, E. Scully, G. D. Tomaras, M. M. Davis, P. Poignard, R. Ahmed, B. D. Walker, B. Pulendran, M. J. McElrath, D. E. Kaufmann, S. Crotty, CXCL13 is a plasma biomarker of germinal center activity, *Proceedings of the National Academy of Sciences* , 201520112–201520112 (2016).

47. Y. Huang, C. Yang, X.-F. Xu, W. Xu, S.-W. Liu, Structural and functional properties of SARS-CoV-2 spike protein: potential antivirus drug development for COVID-19, *Acta Pharmacol. Sin.* **41**, 1141–1149 (2020).

48. G. R. Pullen, M. G. Fitzgerald, C. S. Hosking, Antibody avidity determination by ELISA using thiocyanate elution, *J. Immunol. Methods* **86**, 83–87 (1986).

49. S. Khurana, N. Verma, J. W. Yewdell, A. K. Hilbert, F. Castellino, M. Lattanzi, G. Del Giudice, R. Rappuoli, H. Golding, MF59 adjuvant enhances diversity and affinity of antibody-mediated immune response to pandemic influenza vaccines, *Sci. Transl. Med.* **3**, 85ra48 (2011).

50. M. Narita, Y. Matsuzono, Y. Takekoshi, S. Yamada, O. Itakura, M. Kubota, H. Kikuta, T. Togashi, Analysis of mumps vaccine failure by means of avidity testing for mumps virus-specific immunoglobulin G, *Clin. Diagn. Lab. Immunol.* **5**, 799–803 (1998).

51. K. Bahl, J. J. Senn, O. Yuzhakov, A. Bulychev, L. A. Brito, K. J. Hassett, M. E. Laska, M. Smith, Ö. Almarsson, J. Thompson, A. M. Ribeiro, M. Watson, T. Zaks, G. Ciaramella, Preclinical and Clinical Demonstration of Immunogenicity by mRNA Vaccines against H10N8 and H7N9 Influenza Viruses, *Mol. Ther.* **25**, 1316–1327 (2017).

52. J. L. Schultze, A. C. Aschenbrenner, COVID-19 and the human innate immune system, *Cell* (2021), doi:10.1016/j.cell.2021.02.029.

53. K. Lederer, D. Castaño, D. Gómez Atria, T. H. Oguin 3rd, S. Wang, T. B. Manzoni, H. Muramatsu, M. J. Hogan, F. Amanat, P. Cherubin, K. A. Lundgreen, Y. K. Tam, S. H. Y. Fan, L. C. Eisenlohr, I. Maillard, D. Weissman, P. Bates, F. Krammer, G. D. Sempowski, N. Pardi, M. Locci, SARS-CoV-2 mRNA Vaccines Foster Potent Antigen-Specific Germinal Center Responses Associated with Neutralizing Antibody Generation, *Immunity* **53**, 1281–1295.e5 (2020).

54. L. L. Seifert, C. Si, D. Saha, M. Sadic, M. de Vries, S. Ballentine, A. Briley, G. Wang, A. M. Valero-Jimenez, A. Mohamed, U. Schaefer, H. M. Moulton, A. García-Sastre, S. Tripathi, B. R. Rosenberg, M. Dittmann, The ETS transcription factor ELF1 regulates a broadly antiviral program distinct from the type I interferon response, *PLoS Pathog.* **15**, e1007634 (2019).

55. M. D. Robinson, D. J. McCarthy, G. K. Smyth, edgeR: a Bioconductor package for differential expression analysis of digital gene expression data, *Bioinformatics* **26**, 139–140 (2010).

Acknowledgements

We would like to thank the participants who joined our studies. We would like to thank all of the NYU Vaccine Center staff, including Gali Moritz, Mahnoor Ali, Stephanie Rettig, Heekoung Youn, Brooklyn Henderson, Lisa Zhao, and Harry Lambert for their help in these studies. We thank Maren De Vries for the viral stock production and titration. We thank Meike Dittmann and The Microscopy Laboratory at NYU Langone Health for the use of their microscopes. We thank Ludovic Desvignes for his management of the NYU Langone Biosafety Level 3 laboratory.

Funding

National Institutes of Health grant AI114852 (R.S.H.)
National Institutes of Health grant AI082630 (R.S.H.)
National Institutes of Health grant AI148574 (M.J.M.)
The Microscopy Laboratory at NYU Langone Health is supported in part by NYU Langone Health's Laura and Isaac Perlmutter Cancer Center Support (grant P30CA016087) from the National Cancer Institute Langone.

Author contributions

Conceptualization: M.I.S., A.C., R.S.H., and M.J.M.
Data curation: M.I.S., A.C., S.L.G-G., and R.S.H.
Formal analysis: M.I.S., A.C., S.L.G-G., S.B.K., and R.S.H.

Funding acquisition: M.J.M., and R.S.H.
Investigation: M.I.S, A.C., J.R.A, S.L.G-G., T.K., J.P.W., S.W.H., M.T., R.S.H.
Methodology: M.I.S., A.C., and R.S.H.
Project administration: M.I.S. and R.S.H.
Supervision: R.S.H. and M.J.M.
Validation: M.I.S., S.L.G-G, A.C., and R.S.H.
Visualization: R.S.H.
Writing – original draft: M.I.S. and R.S.H.
Writing – review & editing: M.I.S., A.C., S.L.G-G., S.B.K.,J.P.W., T.K., M.T., M.J.M., S.H., and R.S.H.

Competing interests

MJM reported potential competing interests: laboratory research and clinical trials contracts with Lilly, Pfizer (exclusive of the current work), and Sanofi for vaccines or MAB vs SARS-CoV-2; contract funding from USG/HHS/BARDA for research specimen characterization and repository; research grant funding from USG/HHS/NIH for SARS-CoV-2 vaccine and MAB clinical trials; personal fees from Meissa Vaccines, Inc. and Pfizer for Scientific Advisory Board service.

Figures:

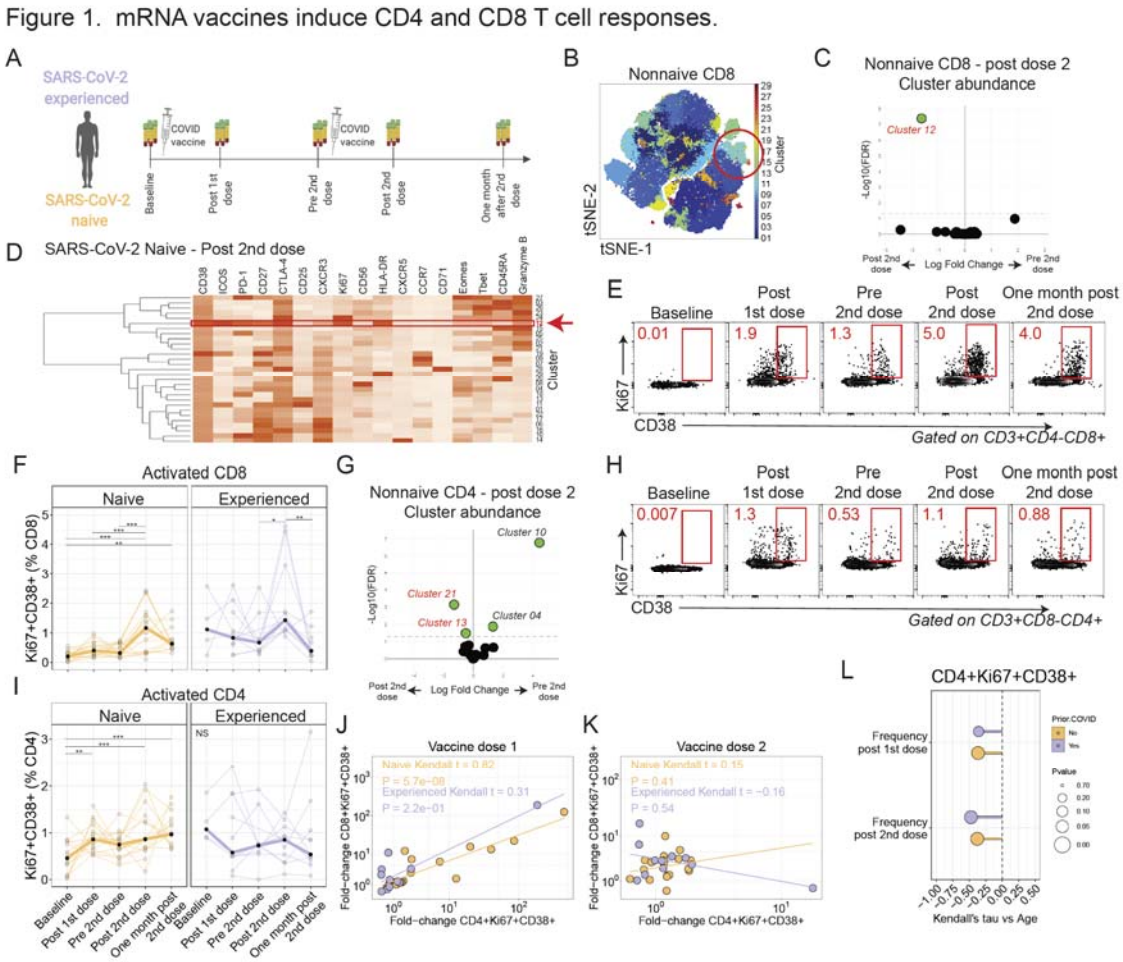

Fig. 1. mRNA vaccination induces CD4 and CD8 T cell responses.
(**A**) Study schematic. (**B**) Non-naive CD8 T cells from all participants were colored using Phenograph clusters and projected using tSNE. Circled region indicates cluster 12. (**C**) Phenograph cluster abundance for non-naive CD8 T cells was compared using edgeR for all participants before and after the second vaccination. (**D**) Heatmap for non-naive CD8 T cell cluster protein expression for SARS-CoV-2-naive participants after the second vaccination. (**E**) Example of CD8 T cell expression of Ki67 and CD38. (**F**) Summary data for Ki67+CD38+ expression in CD8 T cells by cohort. **P*<0.05, ***P*<0.01, and ****P*<0.001. (**G**) Phenograph cluster abundance for non-naive CD4 T cells for all participants before and after second vaccination. (**H**) Example of CD4 T cell expression of Ki67 and CD38. (**I**) Summary data for Ki67+CD38+ expression in CD4 T cells by cohort. ***P*<0.01 and ****P*<0.001. (**J** and **K**) Kendall rank correlations shown for the fold-changes were calculated for CD8+Ki67+CD38+ and CD4+Ki67+CD38+ T cells at one week after first dose compared to baseline (**J**) or at one week after second dose compared to Pre 2ns dose time point (**K**). (**L**) Kendall correlation for the comparison of CD4+Ki67+CD38+ subset versus age. Fold-change Post 1st dose is compared to baseline, and fold-change Post 2nd dose is compared to pre 2nd dose time point. Nominal *p*-values shown.

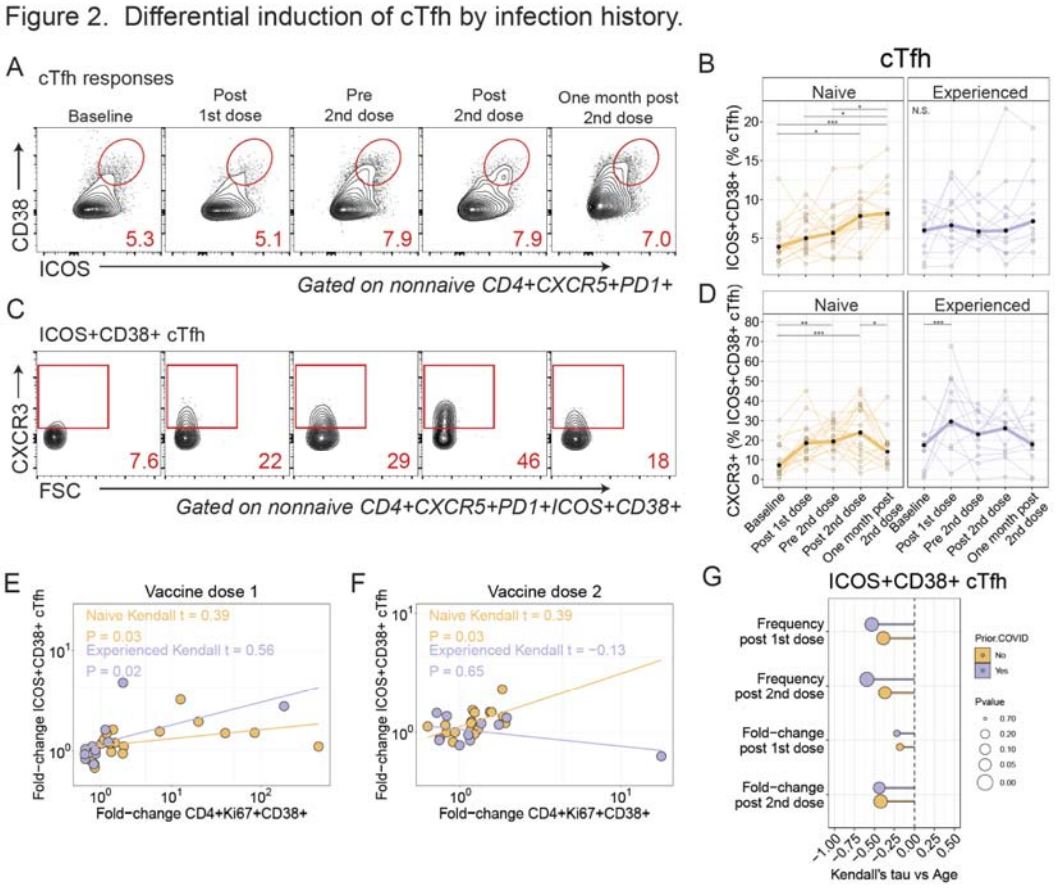

Fig. 2. Differential induction of cTfh responses by COVID-19 history.
(**A**) Example participant shown for ICOS and CD38 in cTfh. (**B**) Summary data for expression of ICOS and CD38 in cTfh. **P*<0.05, ***P*<0.01, and ****P*<0.001. (**C**) Example shown for CXCR3 in ICOS+CD38+ cTfh. (**D**) Summary data for CXCR3 expression in ICOS+CD38+ cTfh. **P*<0.05, ***P*<0.01, and ****P*<0.001. (**E** and **F**) Kendall correlation between the fold-change in ICOS+CD38+ cTfh and Ki67+CD38+ CD4 T cells at one week Post 1st dose compared to baseline (**E**) or one week after second dose compared to Pre 2nd dose (**F**). (**G**) Kendall correlations for the comparison of CD4+Ki67+CD38+ subset versus age. Fold-change Post 1st dose is compared to baseline, and fold-change Post 2nd dose is compared to Pre 2nd dose time point. Nominal *p*-values shown.

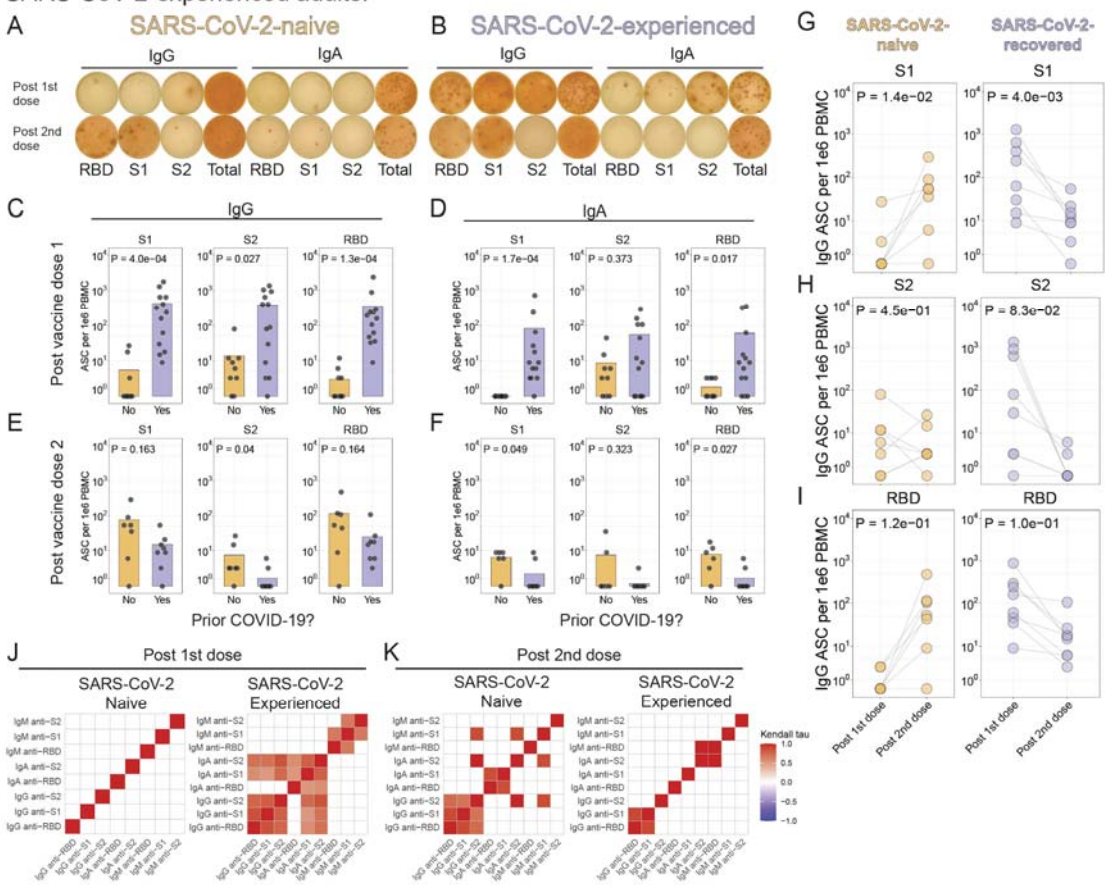

Fig. 3. Few antigen-specific ASC induced in circulation after the second vaccine dose in SARS-CoV-2-experienced adults.
(**A** and **B**). Antibody-secreting cell (ASC) ELISpots for a SARS-CoV-2-naive (**A**) or SARS-CoV-2-experienced (**B**) adult one week after each dose of vaccine. (**C** to **F**) Summary statistics for ELISpot assays. For each panel, S1 (left), S2 (middle), or RBD (right) antigens for IgG or IgA are represented, at one week after first dose (**C** and **D**) or second dose (**E** and **F**). Nominal *P* values from Wilcoxon tests. (**G** to **I**) ELISpot results for SARS-CoV-2-naive (left) or SARS-CoV-2-experienced (right) adults for S1 (**G**), S2 (**H**), or RBD (**I**). Connected lines indicate repeated measurements from the same participants. Nominal *P* values from paired t-tests. (**J** and **K**) Kendall correlations for ELISpot results one week after the first vaccination (**J**) or one week after the second vaccination (**K**). Correlations shown for comparisons with nominal *P* values <0.05.

Figure 4. Antibody responses differ based on prior history of COVID-19.

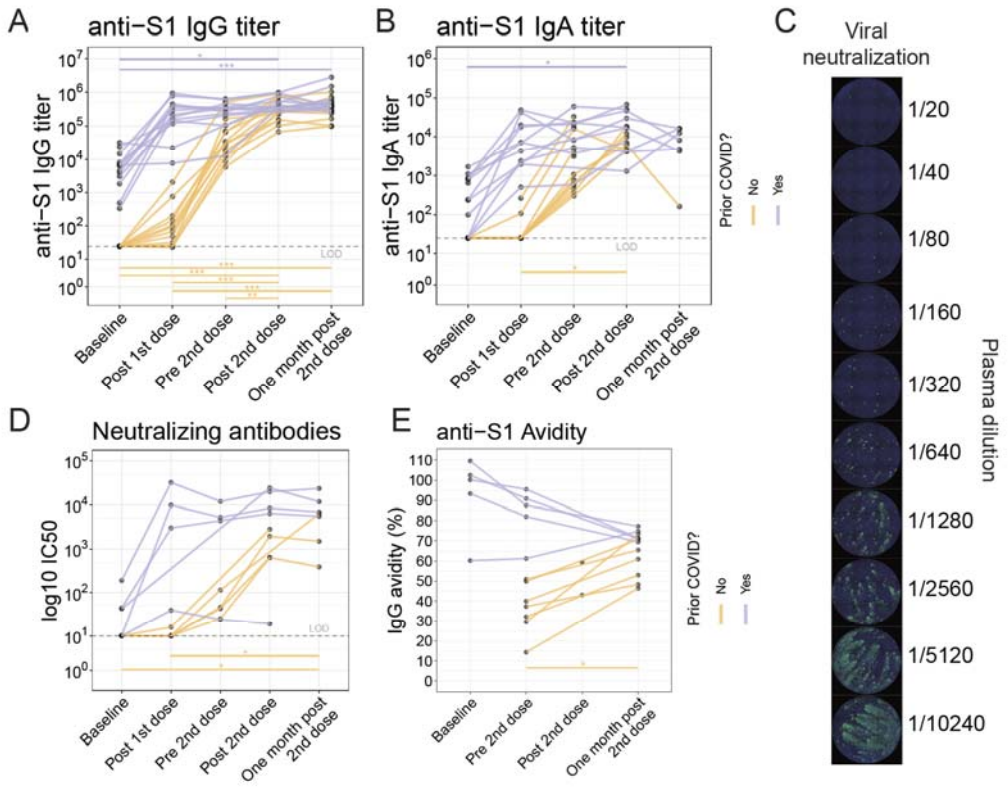

Fig. 4. Antibody responses differ based on prior history of COVID-19.
(**A**) Anti-S1 IgG antibody titers were assessed for SARS-CoV-2 experienced (purple) and SARS-CoV-2-naive (yellow) adults. Connected lines indicate repeated measurements of the same participants. **P*<0.05, ***P*<0.01, and ****P*<0.001. (**B**) Anti-S1 IgA antibody titers. **P*<0.05. (**C**) Neutralizing antibody titers were assessed using an *in vitro* neutralization assay using SARS-CoV-2 virus. Representative dilution series for one subject shown. (**D**) Neutralizing antibody titers shown as $\log_{10}$ IC50. **P*<0.05. (**E**) Anti-S1 IgG antibody avidity assessed using urea wash ELISA. Data expressed as a ratio of urea washed-absorbance to unwashed absorbance. **P*<0.05.

Supplementary Materials

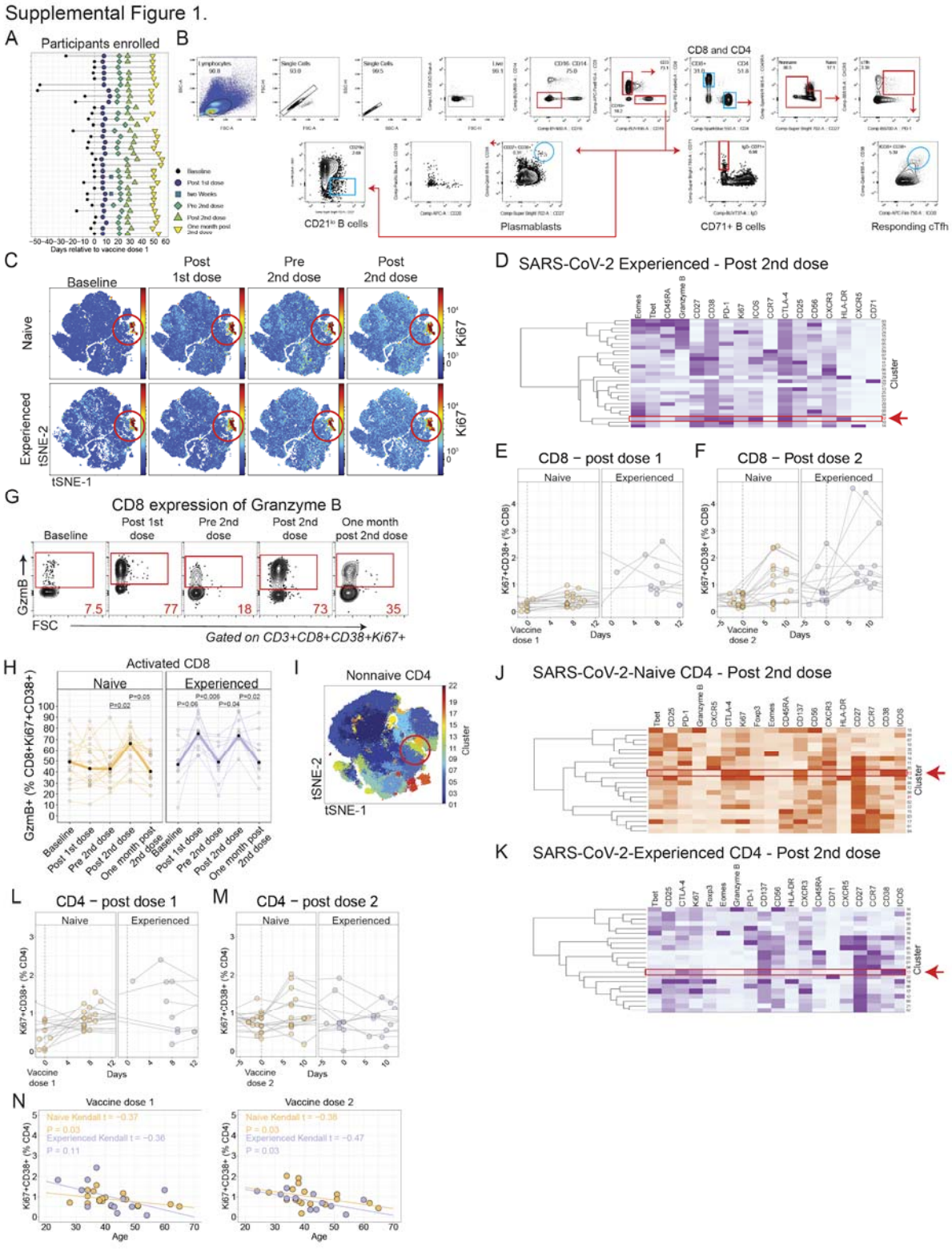

Fig. S1. CD4 and CD8 T cell responses and gating strategy.

(**A**) Study participant timeline relative to first vaccination. (**B**) Gating scheme for T and B cell populations. (**C**) Non-naive CD8 shown in tSNE projection for SARS-CoV-2-naive (upper) or SARS-CoV-2-experienced (lower) participants. Heatmap shows expression of Ki67. Circled area indicates region corresponding to Cluster 12. (**D**) Non-naive CD8 underwent Phenograph clustering. Protein expression for each cluster for SARS-CoV-2-experienced adults shown for samples taken one week after the second vaccination. (**E** and **F**) Ki67+CD38+ expression in CD8 T cells by cohort over time measured in days, relative to the individual's first (**E**) or second (**L**) vaccination. (**G**) Example for Ki67+CD38+ CD8 T cell expression of granzyme B in a SARS-CoV-2-experienced individual. (**H**) Summary data for Ki67+CD38+ CD8 T cell expression of granzyme B. *P*-values from one-way ANOVA with Tukey's post test. (**I**) Non-naive CD4 T cells from all samples were merged for tSNE projection. Colors indicate Phenograph clustering. (**J** and **K**) Protein expression for Phenograph clusters for non-naive CD4 T cells shown for samples at one week following second vaccination in SARS-CoV-2-naive (**J**) or SARS-CoV-2-experienced (**K**) participants. (**L** and **M**) CD4 T cells shown for expression of Ki67 and CD38 after vaccination over time measured in days, relative to the individual's first (**L**) or second (**M**) vaccinations. (**N**) Correlation between Ki67+CD38+ CD4 T cells and age one after either first vaccination (left) or second vaccination (right).

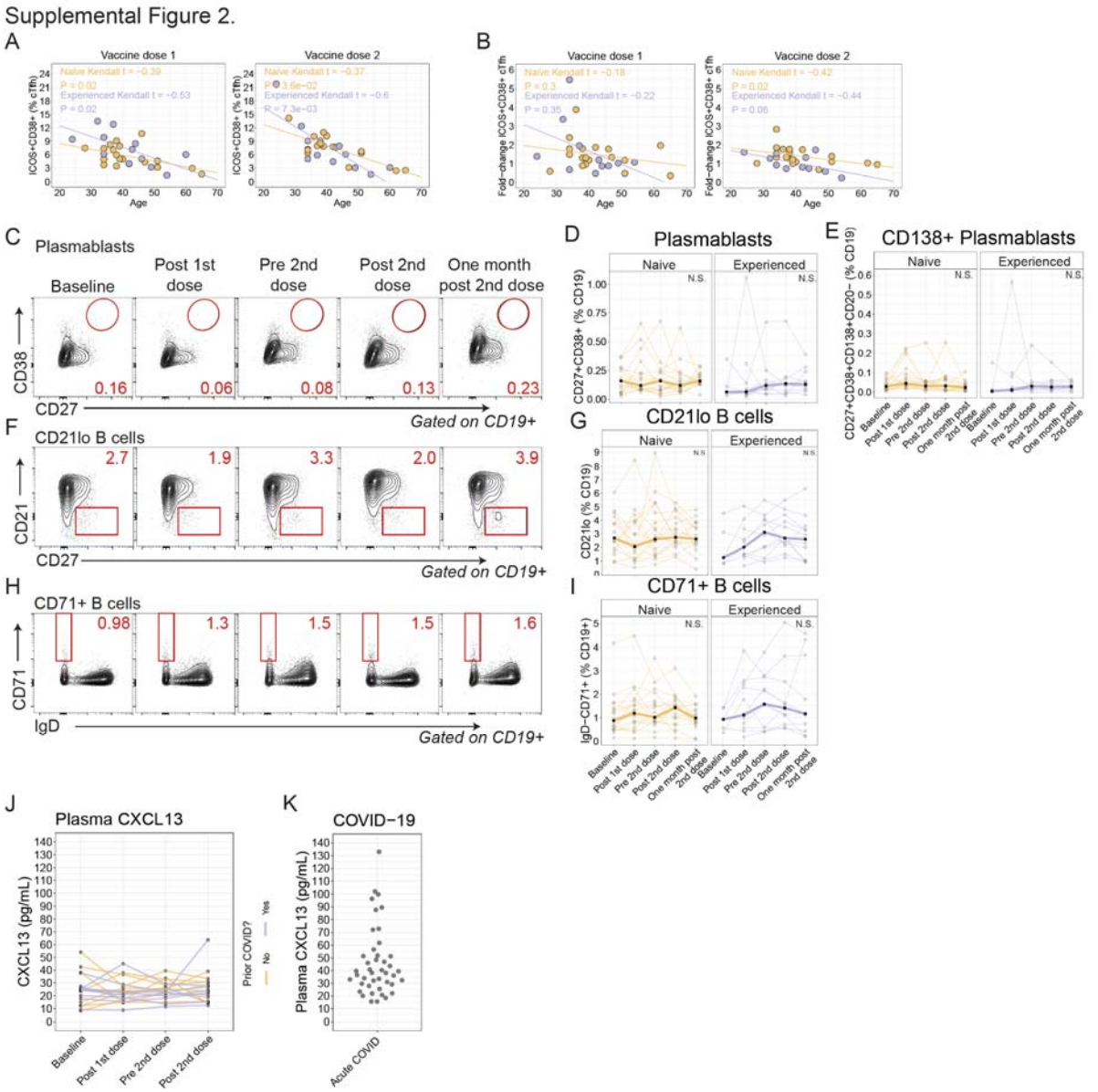

Fig. S2. Plasmablasts and CXCL13 responses to vaccinations.
(**A**) cTfh expressing ICOS and CD38 were negatively correlated with age one week after the first vaccination (left) or the second vaccination (right). (**B**) The fold-change in cTfh expressing ICOS and CD38 at one week after the first vaccination compared to baseline (left) or 1 week after the second vaccination compared to Pre 2nd dose (right) was negatively correlated with age. (**C**) Plasmablasts were identified by expression of CD27 and CD38. Example plot shown. (**D**) Summary data for plasmablasts identified by expression of CD27 and CD38. (**E**) Summary data shown for plasma cells defined as expression of CD27+CD38+CD138+CD20- as a proportion of CD19+ B cells. (**F**) Example plots showing gating for $CD21^{lo}$ B cells. (**G**) Summary data for $CD21^{lo}$ B cells longitudinally. (**H**) Example plots showing gating for CD71+ B cells. (**I**) Summary data for CD71+ B cells longitudinally. (**J**) Plasma CXCL13 shown longitudinally for both

cohorts. (**K**) Plasma CXCL13 in an independent cohort of COVID-19 patients within 30 days of the onset of symptoms.

Supplemental Figure 3.

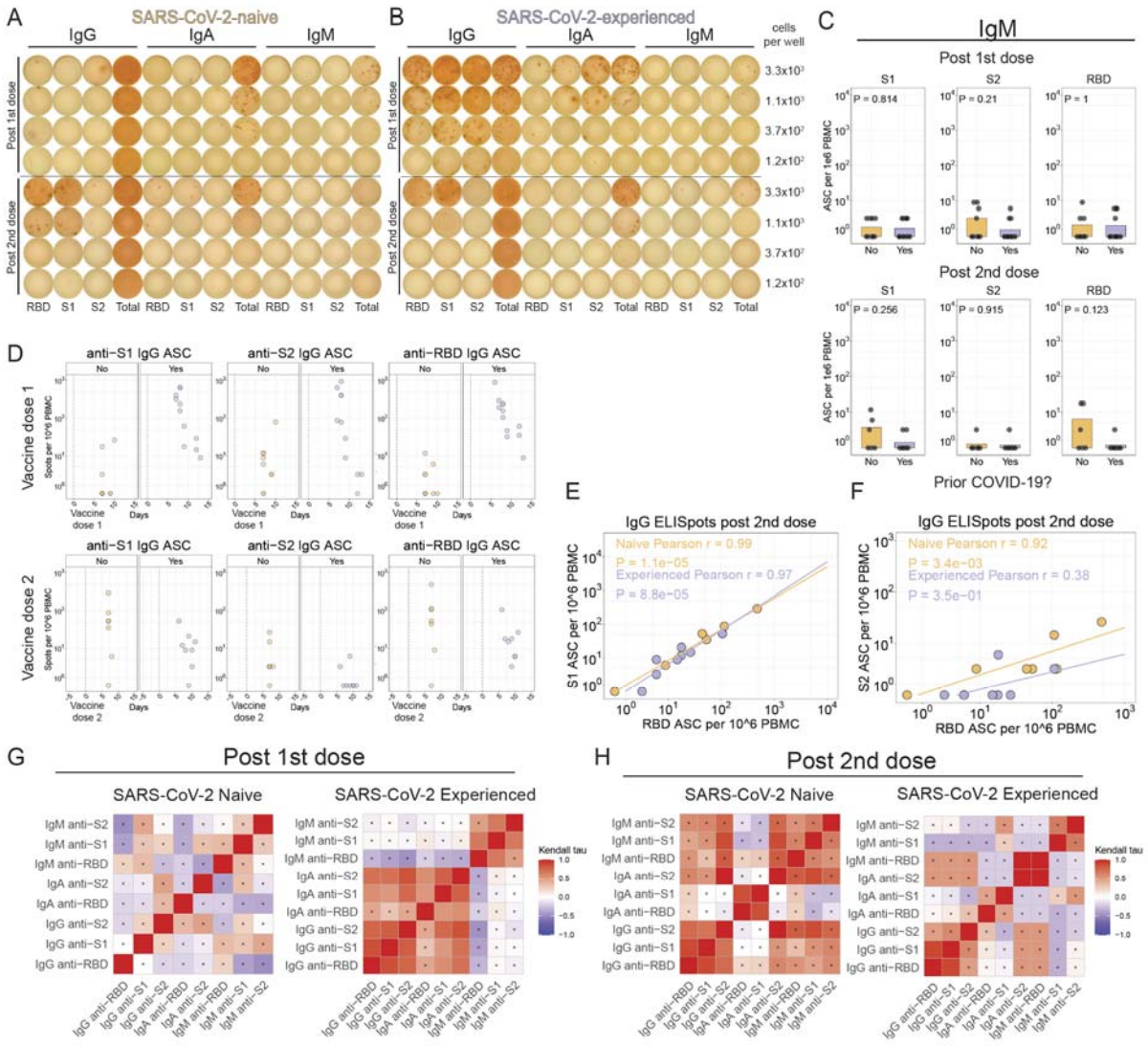

Fig. S3. Poor IgG and IgA ASC responses to second dose in SARS-CoV-2 experienced participants.

(**A** and **B**) Antibody-secreting cell (ASC) ELISpots shown for IgG, IgA, and IgM-producing cells reacting to RBD, S1, or S2 antigens, or total secreted antibody controls. . (**C**) IgM-producing ASC in circulation quantified one week after first vaccination (top) or one week after second vaccination (bottom). Nominal *P* values from Wilcoxon tests. (**D**) ASC frequencies shown over time measured in days relative to the first vaccination (top) or second vaccination (bottom) for S1, S2, or RBD antigens. (**E** and **F**) Correlation shown for both cohorts for S1-reactive IgG ASC (**E**) or S2-reactive IgG ASC (**F**) compared to RBD-reactive IgG ASC one week after second vaccination. (**G** and **H**) Kendall correlation shown for SARS-CoV-2-specific frequencies for SARS-CoV-2-naive or SARS-CoV-2-experienced adults one week after first (**G**) or one week after second (**H**) vaccination. Heatmap colored by Kendall's tau statistic. Boxes with symbols indicate nominal *P* value >0.05.

Supplemental Figure 4.

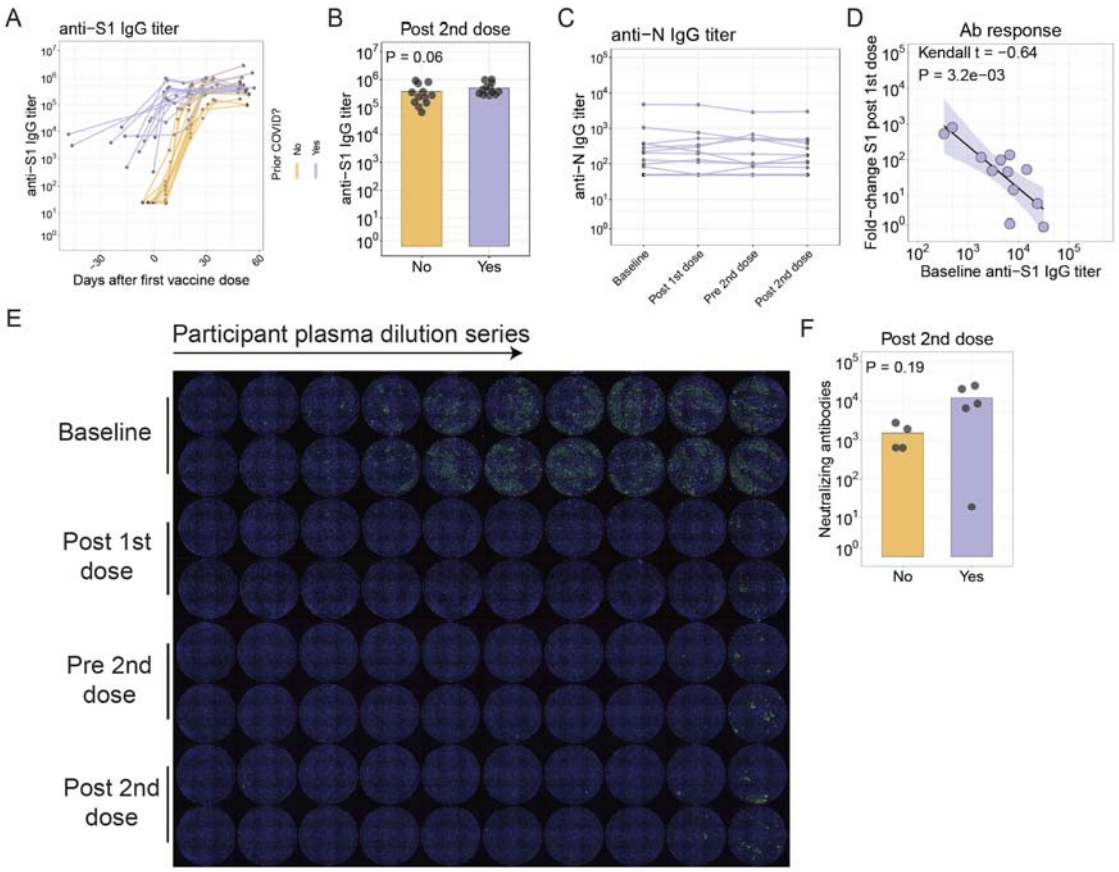

Fig. S4. SARS-CoV-2-experienced individuals' robust anti-S1 binding and neutralizing antibodies responses after vaccination.

(**A**) Anti-S1 IgG serum antibody titers over time measured in days relative to the first vaccination. (**B**) Anti-S1 IgG titer one week after second vaccination for each cohort (*P*=0.06; Wilcoxon test). (**C**) Anti-nucleocapsid IgG serum antibody titers. (**D**) Correlation between fold-change in anti-S1 IgG serum antibody titers, assessed as one week after vaccination compared to baseline, compared to the baseline anti-S1 IgG serum antibody titers, for SARS-CoV-2-experienced adults. (**E**) Example of neutralizing antibody assay shown for the same SARS-CoV-2-experienced participant longitudinally. (**F**) Neutralizing antibody titers one week after the second vaccination (*P*=0.19; Wilcoxon test).

Table S1. Participant demographics.

	SARS-CoV-2-naive	SARS-CoV-2-experienced
Number of participants	19	13
Age		
Median	39	43
Range	28 - 65	24 - 60
Sex (% male)	53%	31%
Race (% Caucasian)	84%	85%
Days since diagnosis of COVID-19		
Median		281
Range		20 – 357

Table S2. Antibodies used for flow cytometry experiments.

Target	Fluorochrome	Clone	Manufacturer	Catalog #
Live/Dead Blue	-	-	Invitrogen	L23105
CD3	APC/Fire 810	SK7	Biolegend	344857
CD4	SparkBlue 550	SK3	Biolegend	344656
CD8	PE-Fire 640	SK1	Biolegend	344761
CD11c	PerCP	Bu15	Biolegend	337234
CD14	BUV805	M5E2	BD	612902
CD16	BV480	3G8	BD	566171
CD19	BUV496	SJ25C1	BD	612939
CD20	APC	2H7	Biolegend	302309
CD21	PE-Cy5	B-ly4	BD	551064
CD23	BUV615	M-L233	BD	751104
CD25	BUV563	2A3	BD	612919
CD27	SB702	O323	Invitrogen	67-0279-42
CD38	Qdot655	HIT2	Invitrogen	Q22150
CD40	BV510	5C3	Biolegend	334330
CD45RA	Spark NIR 685	HI100	Biolegend	304168
CD56	BV570	5.1H11	Biolegend	362539
CD71	SB780	OKT9	Invitrogen	78-0719-42
CD123	BV650	7G3	BD	563405
CD137	PE	4B4-1	Biolegend	309803
CD138	PacBlue	MI15	Biolegend	356531
CD150 (CTLA4)	BV421	BNI3	Biolegend	369606
CD183 (CXCR3)	BV750	1C6	BD	746895
CD185 (CXCR5)	BB515	RF8B2	BD	564624
CD197 (CCR7)	BV605	G043H7	Biolegend	353224
CD278 (ICOS)	APC-Fire750	C398.4A	Biolegend	313536
CD279 (PD-1)	BB700	EH12.1	BD	566460
HLA-DR	BUV661	G46-6	BD	612980
IgD	BUV737	IA6-2	BD	612798
Foxp3	PE-Cy5.5	PCH101	Invitrogen	35-4776-42
Tbet	PE-Cy7	4B10	Biolegend	644823
Eomes	PE-eF610	WD1928	Invitrogen	61-4877-42
GzmB	A700	GB11	BD	561016
Ki67	BUV395	B56	BD	564071
IgG	PerCP-Vio700	IS11-3B2.2.3	Miltenyi	130-119-880